Lancaster, David George; Dawes, J. M.
Methane detection with a narrow-band source at 3.4 μm based on a Nd:YAG pump laser and a combination of stimulated Raman scattering and difference frequency mixing, *Applied Optics*, 1996; 35(21):4041-4045.

Methane detection with a narrow-band source at 3.4 μm based on a Nd:YAG pump laser and a combination of stimulated Raman scattering and difference frequency mixing

D. G. Lancaster and J. M. Dawes

We report the characterization of a 10-Hz pulsed, narrow-band source that is coincident with a fundamental ν_3 rovibrational absorption of methane at 3.43 μm. To generate this midinfrared wavelength, an injection-seeded 1.06-μm Nd:YAG laser is difference frequency mixed with first Stokes light generated in a high-pressure methane cell (1.06 → 1.54 μm) to result in light at a wavelength of 3.43 μm, that is, the ν_1 Raman active frequency of methane (∼2916.2 cm^{-1}). With a modest-energy Nd:YAG laser (200 mJ), a few millijoules of this midinfrared energy can be generated with a pulse width of ∼7 ns (FWHM). The methane ν_1 frequency can be pressure tuned over 8–32 atm (corresponding to ∼13 GHz) and scanned across part of the ν_3 $P(10)$ rovibrational level of methane, resulting in a peak measured methane absorption coefficient of 4.2 cm^{-1} atm^{-1}.

Key words: Methane sensing, difference frequency mixing.

1. Introduction

The ability to monitor methane in the atmosphere is important, as methane is a contributor to the greenhouse effect and a common environmental pollutant. Methane is also a safety hazard in several industries including coal mining, natural gas storage, and the storage and handling of liquefied methane. Optical methods are desirable for methane sensing, as they allow remote operation and the ability to cover a large area with a high sensitivity. The electronics, optics, and data processing required for detection and ranging are mature technologies[1] although suitable rugged laser sources are scarce. Our research is aimed at developing a convenient, practical source for methane sensing that can be used in a dedicated differential absorption lidar system.

Frequency conversion into the midinfrared by a combination of stimulated Raman scattering (SRS) and difference frequency mixing (DFM) was first proposed (and demonstrated) in 1966.[2] Recently a Nd:YAG hybrid system (1 Hz) that used a combination of SRS in methane and optical parametric amplification to amplify the 1.54-μm Stokes light with 3.43-μm light being produced as a byproduct was reported.[3] In this paper we present results for a system we have developed to produce narrow-band pulsed light at 3.43 μm in the millijoule energy range by using an injection-seeded single-longitudinal mode (SLM) Nd:YAG pump laser. The system characteristics include a short pulse (∼7 ns), high peak power, 10-Hz operation, narrow bandwidth, slightly tunable wavelength, and a single pump laser.

In a previous paper[4] we demonstrated a broadband Nd:YAG-based laser system for the sensing of methane with an intrinsic wavelength stability and a measured methane absorption coefficient of 1.5 cm^{-1} atm^{-1}. In this paper, by using a narrow-bandwidth pump laser, we generate narrow-band 3.43-μm light with a bandwidth determined by the pressure broadening inherent in the SRS process and we demonstrate a stronger methane absorption coefficient. The technique depends on a spectral coincidence between the peak of the Raman active Q-branch ν_1 vibrational frequency of methane (the SRS frequency of methane) and the infrared active $P(10)$ rotational level of the fundamental ν_3 vibrational band of methane. For atmospheric methane remote sensing, the attractive features of the source

The authors are with the Centre for Lasers and Applications, School of Mathematics, Physics, Computing and Electronics, Macquarie University, New South Wales 2109, Australia.

Received 1 November 1995; revised manuscript received 8 March 1996.

0003-6935/96/214041-05$10.00/0

include eye safety, daylight operation, a high atmospheric transmission, and a strong methane absorption coefficient.

This system is based on two nonlinear processes in series; for reasonable DFM conversion to occur, the SRS must be optimized. For this experiment we are using backward-generated Stokes light that is counterpropagating to the pump as it has a higher degree of spatial coherence compared with the copropagating forward Stokes light. Moreover, the back-propagating Stokes is a phase conjugate of the pump laser.[5]

2. Experimental Apparatus

A schematic of the midinfrared laser system is shown in Fig. 1. The pump laser is a 1.064-μm injection-seeded SLM Nd:YAG laser (Quanta-Ray GCR-170) with a pulse duration of 7 ns (FWHM). The laser is operated at a repetition rate of 10 Hz and has a clipped beam (8.5 mm × 7 mm) in the near field (1.5 m) with a poor spatial profile, as it was running in a higher-order transverse mode during these experiments. The poor transverse mode did not appear to affect the pump laser SLM operation, because the temporal pulse shape as monitored by a fast photodiode showed no evidence of longitudinal mode beating. Approximately 65% of the pump laser light passes through the beam splitter, where it is apertured to a diameter of 3.5 mm to improve the spatial characteristics. After a delay line to ensure temporal overlap of the Stokes and 1.06-μm pulses, this light reaches the $KTiOAsO_4$ (KTA) crystal. The Raman cell is pumped by the 1.06-μm light reflected from the beam splitter, with the light focused into the center of the cell ($L = 1$ m) by a 0.5-m focal-length lens. The Raman cell is configured for backward SRS by use of a dichroic turning mirror (D1) set at 45° (high reflectivity at 1.06 μm and $T \sim 0.9$ at 1.54 μm) that directs the pump light into the cell while allowing the counterpropagating Stokes light to be transmitted. The Stokes light then passes through a $M = 0.5$ telescope and is recombined with the 1.06 μm by a second dichroic mirror (D2). The two collimated beams are aligned to be approximately collinear and to overlap on the KTA crystal.

The nonlinear crystal KTA was selected for its high damage threshold and transmission at 3.4 μm.[6] A recent report of DFM conversion reported efficiencies of up to 50% by the use of KTA in this spectral region.[7] The KTA crystal used is uncoated and has dimensions of 4 mm × 4 mm × 10 mm. Type I phase matching is used for the difference frequency generation, and the crystal is cut in the *ZX* plane ($\phi = 0$) at $\theta = 82.3°$ (We note that the more established material $KTiOPO_4$, an isomorph of KTA, is unsuitable as it has an absorption near 3.4 μm).

To separate the 3.43-μm light spatially, noncollinear phase matching is used. The two beams (DFM pump and signal) are set at an angle of ~0.5° to each other and spatially overlapped on the front face of the KTA crystal. The generated 3.43-μm light is then separated from the 1.06- and 1.54-μm beams by an angle of ~1.5°. The DFM energy is measured with a calibrated pyroelectric detector (Molectron J3-09).

The cell used for methane transmission measurements is 30 cm long with sapphire windows. A 45° CaF_2 plate reflects a fraction of the incident energy onto a pyroelectric detector, and another pyroelectric detector measures the energy transmitted through the cell. The cell transmission for each pulse is calculated by a ratio of the incident and the transmitted pulse energies that are recorded simultaneously by computerized data acquisition. Transmission is normalized by division by a ratio of the incident and the transmitted pulse energy with no methane in the cell.

3. Results and Discussion

A. Stimulated Raman Scattering

Figure 2(a) shows the backward-generated first Stokes energy as a function of methane pressure for a pump energy of 92 mJ. As can be seen, the Raman conversion efficiency to the backward-generated first Stokes wavelength increases with methane pressure over the range measured, reaching a 5.6% conver-

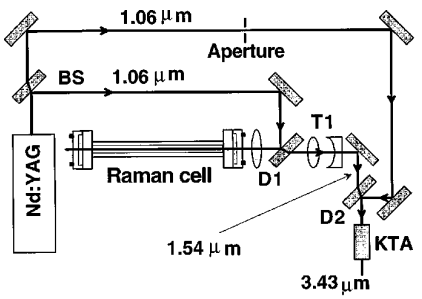

Fig. 1. Schematic of the experimental setup for Raman generation and DFM. The pump is 1.064 μm and the signal is 1.54 μm generated by a backward-configured 1-m methane Raman cell. D1 and D2 are 45° dichroic mirrors with high reflectivity at 1.064 μm and high transmission at 1.54 μm. T1 is a beam-reduction telescope (2×). BS is a beam splitter with a 65% transmission.

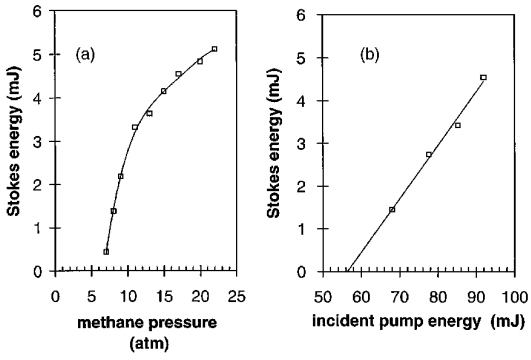

Fig. 2. (a) First Stokes energy as a function of methane pressure in the Raman cell for a 1.06-μm pump energy of 92 mJ (10 Hz), (b) first Stokes energy at a methane pressure of 17 atm (10 Hz) as a function of 1.06-μm pump energy.

sion efficiency at 22 atm. Figure 2(b) shows the slope efficiency for the backward-generated first Stokes light as a function of 1.06-μm energy at a methane pressure of 17 atm. The first Stokes energy increases linearly for increasing pump energies in the range 70–90 mJ with a measured threshold of 56 mJ and a slope efficiency of 13%. Note that corrections were made for losses in the optics, so the data reflect the Stokes energy at the exit of the Raman cell and the pump energy at the entrance to the cell.

For these experiments the 1.06-μm light is focused into the Raman cell with a 0.5-m focal-length lens. Using a shorter lens with increased focal-plane intensities causes periodic sparking or breakdown of the methane gas for this single-pass process. The gas breakdown (especially for backscattered Stokes) is difficult to detect in SRS experiments directly, but causes a spectral jitter in the output of the DFM stage, which is seen as increased noise in the methane spectroscopy experiments.

Back Brillouin scattering of the pump wavelength is also observed and found to increase with methane pressure. A 1.7-m delay line between the pump laser and the Raman cell is used to avoid interference of the backscattered Brillouin light with the SLM mode structure of the pump laser. It should also be noted that polarization is preserved for the first Stokes shift in methane because of the symmetry of the ν_1 vibration (symmetrical stretch), which is important as the DFM phase matching is sensitive to polarization.

We also note that in preliminary work in which a multimode Nd:YAG pump laser was used, the 1-Hz Stokes generation had a pulse stability of $2\sigma \sim 20\%$, whereas at 10-Hz operation the stability was $2\sigma \sim 90\%$, making it unsuitable for further wavelength conversion by DFM. However, with the SLM Nd:YAG pump laser, Stokes light at 10-Hz repetition rates can be generated with a reasonable stability ($2\sigma \sim 13\%$), allowing further nonlinear conversion.

B. Difference Frequency Mixing

The slope efficiencies for the DFM energy at 3.43 μm for a laser repetition rate of 10 Hz are shown in Fig. 3. In Fig. 3(a) the energy at the Stokes wavelength is held constant at 2.9 mJ (methane pressure 17 atm) as the 1.06-μm energy is varied (by a half-wave plate–polarizer combination), resulting in a slope efficiency of 0.6%. This corresponds to a photon conversion efficiency of ~2%. In Fig. 3(b) the 1.06-μm energy is held constant at 46 mJ and the Stokes energy is varied (by absorption filters), resulting in a measured slope efficiency of 8.9%. Note that all measured energies have been corrected for Fresnel losses off the uncoated crystal surfaces (~8%) and are 32 shot averages made by a Tektronix TD320 oscilloscope. The amplitude stability of the DFM energy was measured to be $2\sigma \sim 16\%$.

Inconsistent DFM performance arose if the Stokes energy was varied by an adjustment of the Raman cell pump energy because the spatial or temporal characteristics of the Stokes pulse changed. The DFM conversion depends critically on the coupling of the signal and the pump fields in the KTA crystal. Operation of the Raman conversion process at 10-Hz repetition rate leads to strong thermal effects in the Raman gas, and this, in combination with the poor spatial pump beam quality, means that changes in the Stokes pump energy cause subtle changes in the Stokes beam and thus in the coupling of the fields.

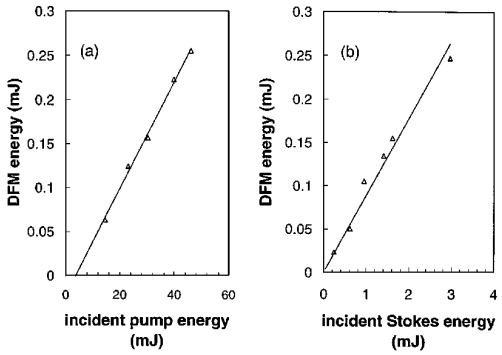

Fig. 3. (a) 3.43-μm pulse energy at 10 Hz as a function of 1.06-μm pulse energy, Stokes energy 2.9 mJ; (b) 3.43-μm pulse energy at 10 Hz as a function of Stokes pulse energy, 1.06 μm = 46 mJ.

The slope efficiencies in Fig. 3 show that the DFM generation is more sensitive to the Stokes (seed) energy than it is to the 1.06-μm energy for the low pulse energies used. Hence, when the seed energy is increased, the 1.06-μm conversion efficiency to 3.43 μm is expected to increase. Furthermore, an increase in crystal length would improve the conversion efficiency, as we are working in a low-energy regime.

The rather low slope efficiency can be attributed to the poor spatial beam quality of the pump laser and the SRS stage of the system. Studies of SRS in methane as a function of repetition rate[8] have concluded that 10-Hz operation leads to substantially poorer beam quality than at lower repetition rates because of the formation of a thermal gradient in the interaction region. We are currently working on methods to improve this apparent deficiency in SRS conversion to allow efficient operation at higher repetition rates. There have also been reports of relaxation oscillation formation, which modifies the Stokes temporal pulse shape.[3,9] This leads to decreased temporal overlap of the two beams incident upon the mixing crystal.

In addition, for these slope efficiency experiments, the spatial overlap between the two beams is not optimized for any one Stokes pressure or Stokes energy. The optimum DFM alignment used in these experiments required that the 1.06-μm spot size be larger than the Stokes spot on the KTA crystal. This tended to compensate for the changing Stokes characteristics as pressure and Stokes energy varied. The mixing alignment was held constant for the methane spectroscopy measurements (for which the DFM wavelength is tuned as a function of methane

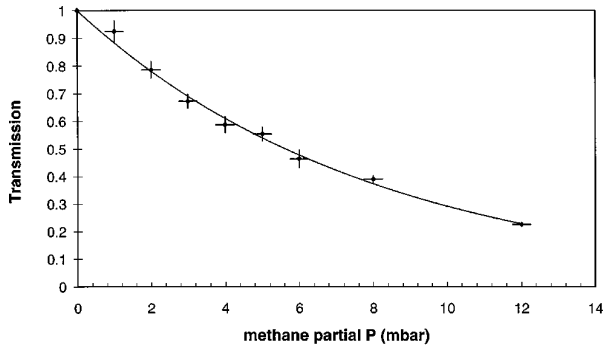

Fig. 4. Transmission of the 3.43-μm (pressure of the methane cell 23 atm) through varying partial pressures of methane in air with a total cell pressure of 1 atm. The absorption cell is 30 cm. The measured absorption coefficient is 4.16 cm^{-1} atm^{-1}. Shown also is an exponential fit to the data.

pressure). When the spot sizes are optimized for a specific Raman pressure we have measured a 7% photon conversion efficiency from the 1.06-μm energy incident upon the KTA crystal to 3.43 μm. Other work[7] has shown the conversion efficiency to 3.43 μm can be substantially improved with a better beam quality pump laser.

C. Methane Detection

To demonstrate the spectral coincidence of the generated light and the ν_3 rovibrational band of methane, we show in Fig. 4 the transmission of the 3.43-μm light as a function of methane partial pressure in 1 atm of air. For this experiment, the Raman output was pressure tuned to produce the highest absorption in the methane transmission cell. The transmission shows the characteristic Lambert–Beer exponential absorption dependence (note the exponential curve fitted to the data). The absorption coefficient is measured to be 4.16 ± 0.21 cm^{-1} atm^{-1}, which agrees well with an absorption coefficient of 4.17 cm^{-1} atm^{-1} calculated from spectroscopic measurements of the $P(10)$ rotational absorption in the ν_3 band of methane.[10] Note that each transmission point is an average of approximately 60 shots; error bars represent the standard deviation ($\sigma \sim 4\%$).

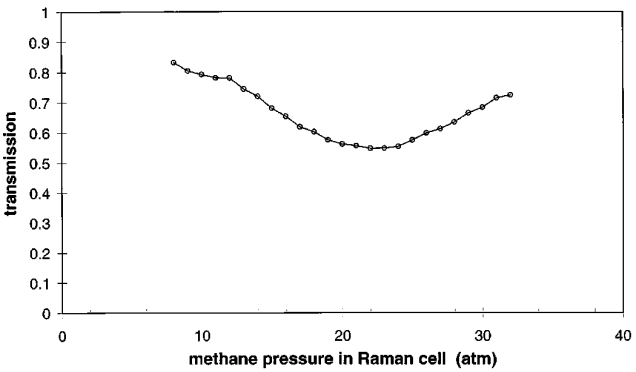

Fig. 5. 3.43-μm transmission through 5 mbars of methane in 1 atm of air for a methane pressure range of 8–32 atm in the Raman cell.

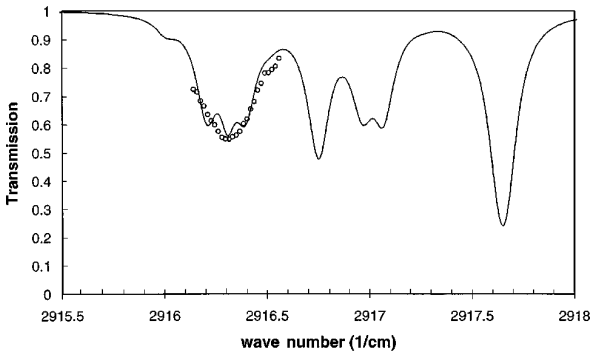

Fig. 6. 3.43-μm transmission through 5 mbars of methane in 1 atm of air. The methane pressure in the Raman cell has been converted into an equivalent wave-number scale, which corresponds to the pressure frequency relation for the ν_1 branch of methane.[11,12] Overlayed is a simulated spectrum of the methane $P(10)$ ν_3 rovibrational band for the same experimental conditions.[13]

Figure 5 shows the normalized transmission of the 3.43-μm light through a cell with a methane partial pressure of 5 mbars in 1 atm of air for a Raman methane pressure range of 8–32 atm. In Fig. 6 the methane pressure (in the Raman cell) has been converted into an equivalent wave-number (in inverse centimeters) shift by the use of a pressure wavelength relation of -0.0175 cm^{-1}/atm.[11] Hence the above Raman-cell pressure range corresponds to tuning over 0.42 cm^{-1} (~13 GHz). Also, at 1-atm methane pressure the Raman shift occurs at the peak of the ν_1 line shape (2916.72 cm^{-1}).[12] Overlaid on this pressure-tuned spectrum is a simulated transmission spectrum of the methane ν_3 $P(10)$ rovibrational absorption for the same partial pressure in air and cell length used in this experiment.[13] As can be seen, there is good agreement between the absolute transmission measured by the tuning of the Raman output and the high-resolution simulated methane transmission spectrum, although the former does not resolve the finer structure in the methane spectrum. If the bandwidth of the SLM pump laser (~0.004 cm^{-1}) is conserved these spectral features should be apparent. The broadening of the DFM bandwidth can be attributed to the pressure broadening inherent for SRS in a pressurized gas medium.[14,15] For methane the spontaneous Raman line shape is proportional to pressure[16] ($\Delta\nu_{\text{spon Ram}} = 0.32 + 0.012$ cm^{-1}/atm) (0.62 cm^{-1} at 25 atm); however, the high gain of the stimulated Raman effect leads to a gain narrowing of the SRS bandwidth. If a simple amplification model of gain narrowing[17] is used and a Lorentzian line shape is assumed, the estimated SRS bandwidth is[15]

$$\Delta\nu_{\text{SRS}} = \Delta\nu_{\text{spon Ram}}\left[\frac{\ln 2}{\ln(G_{\text{SRS}}/2)}\right]^{1/2},$$

where G_{SRS} is the SRS gain. Assuming an amplification of $G_{\text{SRS}} \sim e^{30}$ (threshold condition) this model gives a predicted SRS bandwidth of $\Delta\nu_{\text{SRS}} \sim$

$0.15\Delta\nu_{\text{spon Ram}}$. Hence a methane pressure range of 8–32 atm corresponds to an estimated SRS bandwidth of 0.06 cm^{-1} at the lowest Raman pressure and 0.11 cm^{-1} for the highest pressure.

4. Summary and Conclusions

The light generated by this technique, with its automatic frequency reference and tunability, has several possible uses in remote sensing of methane. The ability to generate a wavelength close to, but not absorbed by, the methane resonance is important for a practical differential absorption lidar system. With our scheme, with a Raman pressure of ~47 atm (in a second cell), light at 2915.9 cm^{-1} would be generated and methane at a partial pressure of 5 mbars in air (for example) would have an absorption coefficient of 0.3 cm^{-1} atm^{-1}, which makes this suitable as an off wavelength. At this stage we have not generated this higher-pressure Stokes wavelength because of the increasing gain of the stimulated Brillouin scattered light that competes with the SRS process (Brillouin energy feeding back into the pump laser could cause damage). It is expected that with further work we can successfully generate this longer wavelength. The second possibility is that the methane detection sensitivity of the system can be set to be appropriate for the expected concentration of the methane present over the chosen remote sensing range. When the Raman methane cell pressure is varied, the wavelength can be chosen so that for higher atmospheric methane concentrations it can be detuned to a lower absorption. Further, this tunability could possibly be used to avoid interfering C–H species in the detection environment.

The research reported here demonstrates a practical method to generate narrow-bandwidth midinfrared light in which the wavelength is set by the Raman medium (in our case methane). Ongoing research is concerned with a more compact system. We have demonstrated a compact in-line Raman oscillator (L = 20 cm) that is resonant at the Stokes wavelength. This has a reduced Stokes threshold energy (18 mJ), which reduces the competition from stimulated Brillouin scattering, and a slope efficiency of ~40% (at 10 Hz). Moreover, with improved pump beam quality we would conservatively expect the DFM conversion efficiency to increase to 10%. Using this Raman oscillator with an optoisolator would give a compact system with reduced pump laser energy requirements so that a small compact flash-lamp-pumped system or perhaps a diode-pumped system would be suitable.

In this paper we have characterized the two nonlinear stages of our system, SRS scattering and DFM. Using these two nonlinear processes in series with a single pump laser, we have demonstrated narrow-bandwidth midinfrared light that is in the millijoules range, at a repetition rate of 10 Hz and with a pulse width of ~7 ns. With this source we have measured a methane absorption coefficient of 4.2 cm^{-1} atm^{-1}, which agrees well with spectroscopic data. We have also demonstrated tuning of the 3.43-μm light by pressure tuning across ~13 GHz of the $P(10)$ rovibrational line of methane.

We acknowledge B. J. Orr for the loan of the SLM Nd:YAG laser used for these experiments. We thank D. J. W. Brown, B. J. Orr, H. Pask, and J. A. Piper for helpful discussions. D. G. Lancaster also acknowledges the Australian government for an Australian Postgraduate Research Award (Industry) scholarship as well as the BHP Company for financial support.

References

1. R. M. Measures, *Laser Remote Sensing* (Wiley, New York, 1984).
2. M. D. Martin and E. L. Thomas, "Infrared difference frequency generation," IEEE J. Quantum Electron. **QE-2,** 196–201 (1966).
3. S. K. Wong, P. Mathieu, and P. Pace, "High-energy hybrid Raman optical parametric amplifier eye safe laser source," Appl. Opt. **33,** 1686–1690 (1994).
4. D. G. Lancaster and J. M. Dawes, "A pulsed laser source using stimulated Raman scattering and difference frequency mixing: remote sensing of methane in air," Opt. Commun. **120,** 307–310 (1995).
5. W. K. Bischel, "Applications of injection-locked Nd:YAG lasers in stimulated Raman scattering," Laser Focus **22**(11), 70–75 (1986).
6. W. R. Bosenberg, L. K. Cheng, and J. D. Bierlein, "Optical parametric frequency conversion properties of $KTiOAsO_4$," Appl. Phys. Lett. **65,** 2765–2767 (1994).
7. A. H. Kung, "Efficient conversion of high-power narrow-band Ti:sapphire laser radiation to the midinfrared in $KTiOAsO_4$," Opt. Lett. **20,** 1107–1109 (1995).
8. Z. Chu, U. N. Singh, and T. D. Wilkerson, "A self seeded SRS system for the generation of 1.54 μm eye-safe radiation," Opt. Commun. **75,** 173–178 (1988).
9. V. Nassisl, C. Padula, and A. Pecoraro, "The effect of CH_4 pressure on backward stimulated Raman scattering generated by a XeCl laser," Opt. Commun. **19,** 267–270 (1993).
10. A. S. Pine, "High-resolution methane ν_3-band spectra using a stabilized tunable difference-frequency laser system," J. Opt. Soc. Am. **66,** 97–108 (1976).
11. A. D. May, J. C. Stryland, and H. L. Welsh, "Raman spectra of H_2 and CH_4 at high pressures," J. Chem. Phys. **30,** 1099–1100 (1959).
12. A. Owyoung, "CW stimulated Raman spectroscopy," in *Chemical Applications of Nonlinear Raman Spectroscopy,* A. B. Harvey, ed. (Academic, New York, 1981), p. 313.
13. *USF Hitran 92 Optical Spectroscopy Database* (University of Southern Florida, Tampa, Fla., 1994).
14. D. V. Guerra and R. B. Kay, "Stimulated Raman scattering in hydrogen pumped with a tunable, high power, narrow linewidth alexandrite laser," J. Phys. B **26,** 3975–3989 (1993).
15. R. Sussmann, Th. Weber, E. Riedle, and H. J. Neusser, "Frequency shifting of pulsed narrow-band laser light in a multipass Raman cell," Opt. Commun. **88,** 408–414 (1992).
16. Y. Taira, K. Ide, H. Takuma, "Accurate measurement of the pressure broadening of the ν_1 Raman line of CH_4 in the 1–50 atm region by inverse Raman spectroscopy," Chem. Phys. Lett. **91,** 299–302 (1982).
17. A. E. Siegman, *Lasers* (University Science, Mill Valley, Calif., 1986), p. 281.